OPEN ACCESS

TRANSLATIONAL SCIENCE

CD19-targeting CAR T cells protect from ANCA-induced acute kidney injury

Dörte Lodka,[1] Maria Zschummel,[2] Mario Bunse,[2] Anthony Rousselle,[1] Janis Sonnemann,[1,3] Ralph Kettritz,[1,3] Uta E Höpken,[2] Adrian Schreiber [1,3]

Handling editor Josef S Smolen

► Additional supplemental material is published online only. To view, please visit the journal online (http://dx.doi.org/10.1136/ard-2023-224875).

[1]Experimental and Clinical Research Center, Charité - Universitätsmedizin Berlin and Max Delbrück Center for Molecular Medicine in the Helmholtz Association, Berlin, Germany
[2]Max Delbrück Center for Molecular Medicine in the Helmholtz Association, Berlin, Germany
[3]Department of Nephrology and Medical Intensive Care, Charité - Universitätsmedizin Berlin, Berlin, Germany

Correspondence to
Dr Adrian Schreiber, Charité - Universitätsmedizin Berlin, Berlin, 13125, Germany; adrian.schreiber@charite.de

UEH and AS are joint senior authors.

Received 17 August 2023
Accepted 18 December 2023
Published Online First 5 January 2024

To cite: Lodka D, Zschummel M, Bunse M, *et al*. *Ann Rheum Dis* 2024;**83**:499–507.

ABSTRACT

Objectives Anti-neutrophil cytoplasmic autoantibody (ANCA)-associated vasculitides (AAV) are life-threatening systemic autoimmune diseases manifesting in the kidneys as necrotizing crescentic glomerulonephritis (NCGN). ANCA antigens are myeloperoxidase (MPO) or proteinase 3. Current treatments include steroids, cytotoxic drugs and B cell-depleting antibodies. The use of chimeric antigen receptor (CAR) T cells in autoimmune diseases is a promising new therapeutic approach. We tested the hypothesis that CAR T cells targeting CD19 deplete B cells, including MPO-ANCA-producing B cells, thereby protecting from ANCA-induced NCGN.

Methods We tested this hypothesis in a preclinical MPO-AAV mouse model. NCGN was established by immunisation of MPO$^{-/-}$ mice with murine MPO, followed by irradiation and transplantation with haematopoietic cells from wild-type mice alone or together with either CD19-targeting CAR T cells or control CAR T cells.

Results CD19 CAR T cells efficiently migrated to and persisted in bone marrow, spleen, peripheral blood and kidneys for up to 8 weeks. CD19 CAR T cells, but not control CAR T cells, depleted B cells and plasmablasts, enhanced the MPO-ANCA decline, and most importantly protected from NCGN.

Conclusion Our proof-of-principle study may encourage further exploration of CAR T cells as a treatment for ANCA-vasculitis patients with the goal of drug-free remission.

WHAT IS ALREADY KNOWN ON THIS TOPIC

⇒ Antineutrophil cytoplasmic antibody-associated vasculitis is characterised by severe vascular inflammation and glomerulonephritis. Current therapeutic approaches leave up to 30% of patients with inefficient control of disease activity.

WHAT THIS STUDY ADDS

⇒ We demonstrate that CD19 chimeric antigen receptor (CAR) T cells deplete B cells and plasmablasts in anti-neutrophil cytoplasmic autoantibody-induced glomerulonephritis leading to protection from disease.

HOW THIS STUDY MIGHT AFFECT RESEARCH, PRACTICE OR POLICY

⇒ Use of CD19 CAR T cells could be a novel treatment strategy in human crescentic glomerulonephritis.

INTRODUCTION

Anti-neutrophil cytoplasmic autoantibody (ANCA)-associated vasculitis (AAV) comprises a group of life-threatening systemic autoimmune diseases, most frequently affecting lungs and kidneys.[1] Patients with granulomatosis with polyangiitis and microscopic polyangiitis harbour either ANCA to proteinase 3 (PR3) or myeloperoxidase (MPO). ANCA binding to their target autoantigens expressed by neutrophils and monocytes, activates these myeloid cells leading to subsequent vascular inflammation and injury.[2–4] In addition, adaptive immunity contributes to the disease by generating ANCA but also by T cell-dependent mechanisms.[5] The pathogenicity of MPO-ANCA was firmly established in different animal models, whereas convincing PR3-ANCA models are lacking.[6–8] B cell depletion with rituximab, a monoclonal antibody against the B cell surface marker CD20, is effective in inducing remission in AAV patients, but leaves up to 30% of patients with uncontrolled disease activity.[9–12] Furthermore, approximately 30%–50% of AAV patients experience disease relapses requiring long-term rituximab.[11 13–15]

Chimeric antigen receptor (CAR)-modified T cells have been genetically engineered to recognise the B cell receptor CD19. After successful testing in murine models of B cell malignancies,[16] CD19 CAR T cells were shown to induce long-term disease remission in patients with chemotherapy-resistant follicular lymphoma,[17] acute lymphoblastic leukaemia[18] and chronic lymphocytic leukaemia.[16] These results led to a recent approval of CD19 CAR T products by the US Food and Drug Administration (FDA).

Conceivably, CAR T cell application has therapeutic potential in autoimmune diseases with advantages over an antibody-based rituximab approach. For example, CAR T cells actively migrate into lymphoid organs as well as into primary target organs and persist over prolonged time periods. The efficacy of CD19 CAR T cells was demonstrated in murine models of autoimmune systemic lupus erythematosus (SLE)[19] and recently in treatment-resistant SLE patients.[20 21] Whether or not CAR T cells are effective in autoimmune diseases other than SLE is not known.

We studied feasibility and efficacy of CD19 CAR T cells in a murine MPO-AAV model. We produced a second generation CD19 CAR composed of an extracellular antibody-derived antigen-binding

domain (scFv of mouse CD19-targeting antibody), a transmembrane domain (CD4-derived), an intracellular signalling (CD3ζ-derived) and a costimulatory domain (CD28-derived) that induce T cell activation.[22] We tested the hypothesis that CD19-targeting CAR T cells lead to persistent B cell depletion, thereby protecting mice from MPO-ANCA induced necrotizing crescentic glomerulonephritis (NCGN).

METHODS

Construction of anti-mouse CD19 CARs

The codon-optimised variable heavy and light chain sequences of the rat CD19 hybridoma 1D3 were synthesised and introduced into a murine CAR backbone consisting of an IgG1 spacer (228 aa), a CD4 transmembrane domain and an intracellular CD28 costimulatory domain followed by a CD3ζ activation domain.[22]

Retroviral vector production

Mouse CD19 and SP6 CAR (recognising the hapten 2, 4, 6-trinitrobenzenesulfonic acid, not present in mice[23]) viral supernatants were harvested from stable producer cell lines based on transduced and sorted Platinum-E packaging cells.

Mouse T cell transduction

Splenocytes were isolated from C57BL/6N mice, cultured in T cell medium (TCM: RPMI, 10% FCS, 1 mM NaPyr, 0.1 mM MEM NAA, 100 U/mL penicillin, 100 µg/mL streptomycin) supplemented with 10 ng/mL mouse IL-7 and 50 ng/mL mouse IL15 (both Peprotech) and activated for 1 day on anti-CD3/anti-CD28 mAb-coated plates (1 µg/mL anti-CD3 mAb, 0.1 µg/mL anti-CD28 mAb). For the first transduction on the next day, virus-coated plates were prepared as follows: 24-well non-tissue culture plates were coated with RetroNectin (TaKaRa), 0.5 mL/well viral supernatant was added and the plates were centrifuged at 3800 g for 90 min at 4°C. Afterwards the viral supernatant was removed, the wells were washed and blocked (2% BSA in PBS). The activated splenocytes were resuspended in fresh TCM and 0.5 mL/well were transferred together with 0.5 mL/well of viral supernatant to the plate. IL-7/IL-15 were added, and the plates were centrifuged (800 g for 30 min at 32°C). A second transduction was performed the following day. Five hundred microlitre medium/well were removed, 0.5 mL viral supernatant with cytokines was added and the plates were centrifuged (800 g for 30 min at 32°C). After the second transduction, the T cells were cultured in fresh TCM with cytokines for 3 days. Then, the medium was again renewed, and the cell density adjusted to 1×10^6/mL. The T cells were used for in vivo and in vitro experiments after 6–7 days in culture.

Cytokine release

Retrovirally transduced T cells and untransduced T cells were cultured in TCM for 24 hours in the presence of Eμ-TCL tumour B cells in a 1:1 ratio (5×10^4 cells/well each, 1×10^5 total). IFNγ concentration in the cell-free culture supernatant was measured by ELISA (BD Biosciences), as per the manufacturer's instruction. Maximal release was induced by phorbol myristate acetate (5 ng/mL)/ionomycin (1 µM) stimulation of effector cells and minimum release represents T cells incubated without target cells. The optical density was determined using a PowerWave microplate reader and KC4 V.3.0 software (both Bio-TEK).

Animal experiments

Mice were kept under specific pathogen-free conditions at the Max Delbrück Center for Molecular Medicine (MDC, Berlin, Germany) animal facility. The purification of murine MPO and the immunisation of $Mpo^{-/-}$ mice (MPO gene-deficient C57BL/6 mice) were performed as described previously.[7] In brief, $Mpo^{-/-}$ mice, to whom MPO provides an alloantigen, were immunised intraperitoneally with murine MPO in complete Freund's adjuvant to trigger antibody generation against MPO. An intraperitoneal boost with murine MPO in incomplete Freund's adjuvant after 4 weeks improves the robustness of the immune response. Mice were then irradiated with 900 rad to deplete endogenous leucocytes and their progenitors and to create a bone marrow niche for engraftment of the subsequently transplanted bone marrow or CAR T cells. Animals were intravenously reconstituted with MPO-expressing bone marrow cells (1.5×10^7) from C57BL/6J WT mice alone or additionally with 2×10^6 CAR T cells (SP6 or CD19). Mice were sacrificed 2, 5 or 8 weeks following transplantation as indicated. Animal numbers are listed in online supplemental table 1.

Histological examination of kidney damage

Excised kidneys were collected in cold PBS, fixed in 4% formalin overnight, and embedded in paraffin using routine procedures. Sections (3 µm) were stained with Periodic acid–Schiff reaction and all glomeruli on each kidney section assessed by light microscopy using an Axio Imager M2 microscope (Zeiss, Jena, Germany). Glomerular crescents and necrosis were expressed as the mean percentage of glomeruli with crescents and necrosis in each animal and scored in a blinded fashion. Pictures were taken with the microscope BZ-X810 (Keyence, Neu-Isenburg, Germany).

Functional measurement of kidney damage

Urine samples were collected by housing mice for 16 hours in metabolic cages with free access to water and food. Urinary albumin content was determined by ELISA (Bethyl Laboratories, Montgomery, TX, USA). Urinary creatinine was determined by means of Clinical Chemical Analysis System AU480 (Beckman Coulter). Neutrophil gelatinase-associated lipocalin (NGAL) concentration in urine was determined with the NGAL (LCN2) ELISA Kit from Dianova (Hamburg, Germany).

Anti-MPO-titre determination

Titre determination was performed with ELISA as follows, 96-well microtitre plates were coated with 0.5 µg/well murine MPO, blocked with 1% goat serum in PBS, mouse sera were added, bound anti-MPO antibodies detected with alkaline phosphatase-conjugated goat anti-mouse IgG antibody (Sigma A7434), p-nitrophenylphosphate phosphatase-substrate (Sigma N1891) was added and the colorimetric reaction was analysed by 405 nm (VERSAmax, Molecular Devices). Results were expressed as percentage of a positive control serum pool.

Isolation of leucocytes

Kidney specimens were minced with scissors and digested for 40 min at 37°C with 0.2 mg/mL liberase and 100 U/mL DNase in phosphate buffered saline without magnesium and calcium ions (PBS). Cell suspensions were washed with MACS buffer (PBS/2% BSA/2 mM EDTA), filtered through 70 µm meshes, resuspended in lysis buffer (Sigma-Aldrich) to remove erythrocytes, washed and resuspended in MACS buffer, and further processed for flow cytometry. Spleen specimens and lymph nodes (two inguinal, two brachial, three mandibular per mouse) were rubbed through 70 µm cell strainers with a syringe plunger. Cell suspensions were centrifuged, and further processed like kidney samples. Bone

marrow cells were isolated from femur and tibia (referred to as 'leg' for calculating cells numbers in the results part). The bone ends were cut-off and the bone marrow was rinsed out with PBS using a syringe. Cells were passed through a 70 µm cell strainer, centrifuged and further processed like kidney samples. 200 µL of blood were collected in EDTA-containing tubes. Erythrocytes were lysed by addition of 2 mL ammonium chloride and incubation at 37°C for 5 min. Lysed erythrocytes were removed by centrifugation, cell pellets were resuspended in MACS buffer and used for flow cytometric measurements.

Flow cytometry

Cell suspensions of spleen, bone marrow, lymph nodes, blood and kidney were incubated for 30 min on ice with anti-mouse CD16/32 antibody (Biolegend) to block Fc receptors. Cells were then incubated for 20 min at 4°C with the following fluorochrome-conjugated antibodies for the T cell panel: CD45.1, CD45.2, CD3, CD4, CD8a, CD19 and anti-IgG for the detection of the CAR; for the B cell panel: CD45.2, B220, CD19, CD27, CD38, CD138 and anti-IgG; for the myeloid panel (only used for kidney samples): CD45, CD11b, CD11c, Ly-6G, Ly6c, F4/80, I-A/I-E. Dead cells were excluded using the LIVE/DEAD Fixable Aqua Dead Cell Stain Kit (ThermoFisher Scientific, Rockford, IL, USA) for T and B cell panels and with LIVE/DEAD Fixable Near-IR Dead Cell Stain Kit (ThermoFisher Scientific) for the myeloid panel. For quantification of measured cell numbers CountBright Absolute Counting Beads (Invitrogen) were added to the flow cytometric samples. Flow cytometry measurements were performed using a BD CANTO II and LSR FORTESSA flow cytometer with BD FACSDiva software. Data were analysed using FlowJo Software V.10 (Treestar, Ashland, OR, USA). Antibody details are listed in online supplemental table 2.

RNA isolation, cDNA synthesis, reverse transcription-PCR

Total RNA was extracted with the RNeasy Mini Kit (Qiagen, Hilden, Germany) following the manufacturer's instructions and treated with DNase (Promega, Mannheim, Germany). Complementary DNA was transcribed with RiboLoc and reverse transcriptase following the manufacturer's protocol using the GeneAmp PCR System 9700 V.3.12 (Applied Biosystems). Reverse transcription-PCR (RT-PCR) was performed using fast SYBR Green Mastermix and QuantStudio 5 System with 384-well block (both Applied Biosystems). Each sample was measured in triplicate, and expression levels were normalised to HPRT expression. Primer details are listed in online supplemental table 3.

Statistics

Results are given as means with SD. Comparisons were made using analysis of variance with Kruskal-Wallis analysis for figures 2–4 and online supplemental figures 3–7 and with Mann-Whitney test for figure 1 using GraphPad Prism V.7 software. Differences were considered significant at $p<0.05$ (*) or $p<0.01$ (**).

RESULTS

CD19 CAR T cells engraft in mice with anti-MPO-induced glomerulonephritis

We first explored whether CAR T cells specifically targeting CD19-expressing B cells engraft in a preclinical mouse model of autoimmune NCGN. Anti-MPO ANCA-induced glomerulonephritis was established by a bone marrow transplantation model. We induced antibody-generation against murine MPO in MPO gene-deficient mice by immunisation with native murine MPO in CFA followed by a booster immunisation after 4 weeks. After irradiation, animals were reconstituted with haematopoietic stem cells by intravenous application of bone marrow cells isolated from wildtype C57BL/6 mice. Subsequently, the induced anti-MPO immunity together with the MPO-positivity in the engrafted circulating haematopoietic cells leads to anti-MPO antibody-induced vasculitis and glomerulonephritis. This model allows investigation of the pathogenic role of both the innate and the adaptive immune system and their contribution to the development of renal damage in ANCA-associated NCGN. To enable CAR T cell engraftment, we established a protocol with intravenous transfer of both MPO-positive bone marrow cells and 2×10^6 CAR T cells at day 1 after irradiation. Mice were sacrificed at three different time-points after CAR T treatment (2, 5 and 8 weeks after cell transfer) to monitor CAR T cell engraftment in different compartments over an 8-week time period (figure 1A).

We developed a second-generation mouse CD19 CAR consisting of a single chain variable fragment recognising mouse CD19, an IgG1 spacer, a CD4-derived transmembrane domain, and intracellular signalling domains originating from CD28 and CD3ζ (figure 1B). SP6 CAR T cells, recognising an irrelevant antigen that is not present in mice served as control. CD19 and SP6 CAR T cells showed a transduction efficacy of 40%–50% (figure 1C) and were used at day 5 of expansion for in vitro analysis (figure 1D) and in vivo transfer (figure 1A). Three groups of animals were compared, namely mice without transfer of CAR T cells (control), mice transferred with SP6 CAR T cells and mice transferred with CAR T cells targeting CD19, respectively. CAR T cell migration and engraftment in spleen, bone marrow, lymph nodes, peripheral blood and kidneys were detected by flow cytometry in both CAR T cell groups. The gating strategy is depicted in online supplemental figure 1. CAR T cells were identified as being double positive for CD3 and the anti-IgG hinge region of the CAR construct. A dot plot representation of CAR T cells in the spleen is shown in figure 1E. Engraftment of SP6 and CD19 CAR T cells in spleens as a major lymphoid organ were already detectable 2 weeks after cell transfer (online supplemental tables 4 and 5 show mean and p values, respectively). Splenic SP6 and CD19 CAR T cell numbers initially decreased from the 2-week to the 5-week time-point and remained stable thereafter until 8 weeks. CAR T cells were also detected in the bone marrow with cell numbers being similar at all analysed time-points. In lymph nodes and peripheral blood, CAR T cells were found at all time-points (figure 1F). Additionally, CAR T cells temporarily appeared in the kidneys as the primary AAV-target organ. This CAR T cell influx was most evident in the early acute phase of the disease course at 2 weeks and decreased gradually at 5 and 8 weeks (figure 1F). The flow-cytometry data of CAR T cell engraftment was confirmed by quantification of CAR construct mRNA by RT-PCR (figure 1G and online supplemental figure 1).

Taken together, we observed stable engraftment of transferred CAR T cells in different lymphoid organs over a time period up to 8 weeks after transfer, and transient appearance in the kidneys.

CD19 CAR T cells deplete B cells in mice with anti-MPO-induced glomerulonephritis

We next asked whether CD19 CAR T cells efficiently deplete B cells in mice with anti-MPO-induced glomerulonephritis. Both

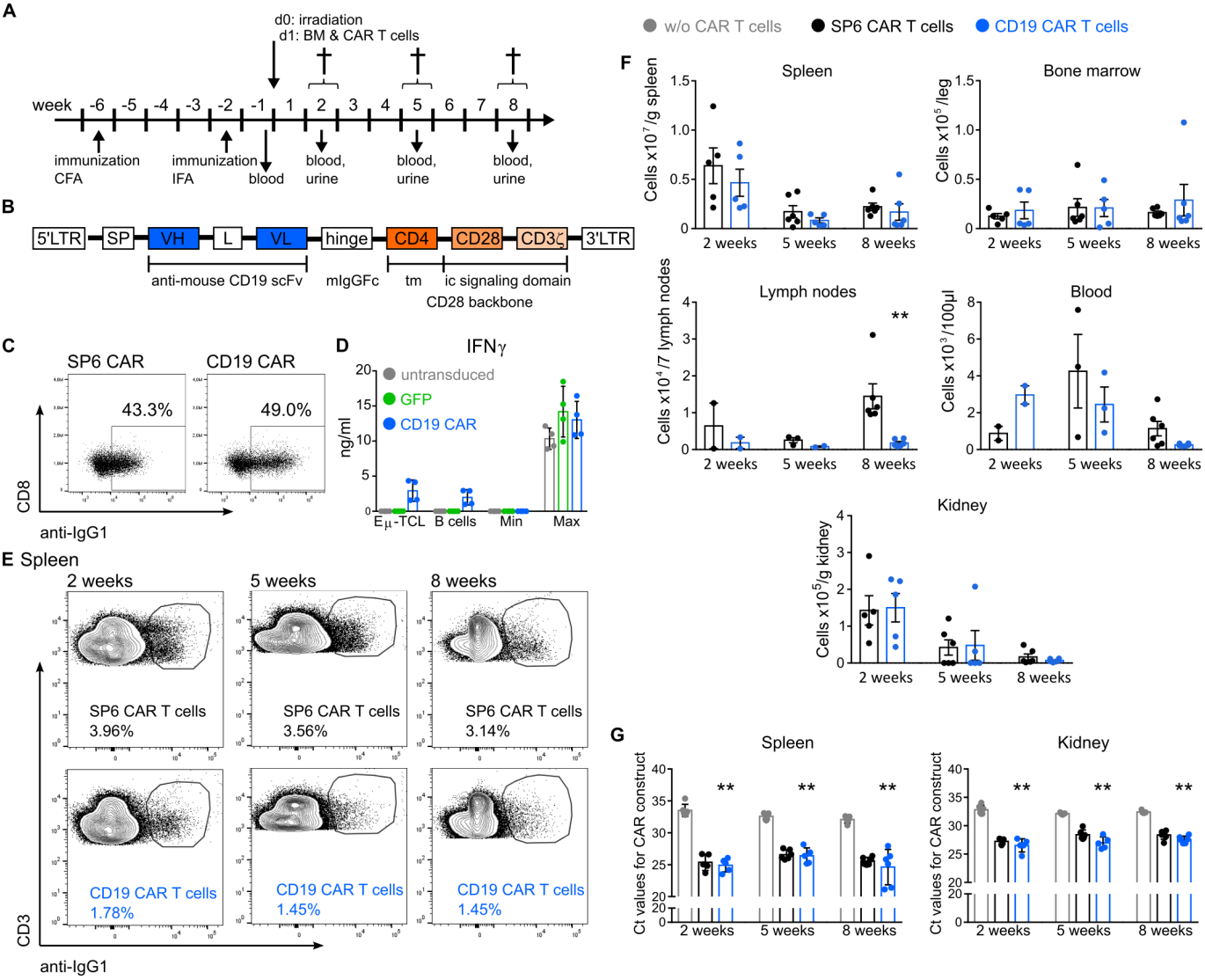

Figure 1 CD19 CAR T cells stably engraft in mice with anti-myeloperoxidase (MPO) induced glomerulonephritis. (A) Experimental procedure of anti-MPO induced glomerulonephritis. The disease was induced by immunisation of $MPO^{-/-}$ mice with murine MPO and subsequent irradiation and wild-type bone marrow (BM) transplantation. CAR T cells (2×10^6) were simultaneously injected with BM cells (1.5×10^7). (B) Schematic of the anti-mouse CD19 chimeric antigen receptor (CD19 CAR). (C) Mouse splenic T cells were transduced with CD19 CAR or control SP6 CAR. CAR surface expression was detected by anti-CD8 and anti-IgG costaining and percentages of CAR^+-T cells are indicated ($CD8^+$ and $CD8^-$). (D) Mouse splenic T cells (5×10^4) were let untransduced or transduced with the mouse CD19 (CD19) CAR or GFP (the same viral vector backbone) and cocultured for 24 hours in a 1:1 ratio with primary murine Eμ-TCL tumour B cells ($CD19^+$) or splenic $B220^+$ B cells. As activation marker, IFNγ in the supernatant was quantified by ELISA. Data of n=2 independent experiments are shown. (E) Representative flow-cytometry analysis displaying engraftment of CAR T cells in the spleen of SP6 and CD19 CAR-treated mice at 2, 5 and 8 weeks detected by anti-IgG and anti-CD3 costaining. (F) Flow cytometric quantification of CAR T cells in different lymphoid compartments and the kidneys of SP6 and CD19 CAR-treated mice at 2, 5 and 8 weeks. (G) Real-time PCR analysis of CAR constructs in spleen and kidneys. Ct values as measure for CAR presence were depicted. Ct values higher than 30 are considered negative. Data in (D), (F) and (G) are represented as individual values and averages with SD. Difference between SP6 and CD19, *p<0.05, **p<0.01. Two independent experiments with a total of 5–7 mice per group were done. CAR, chimeric antigen receptor; CFA, complete Freund's adjuvant; ic, intracellular; IFA, incomplete Freund's adjuvant; L, Whitlow linker; LTR, long terminal repeat; Max, maximal IFNγ-secretion by CAR T cells induced by Phorbol-12-myristate-13-acetate/Ionomycin; Min, minimal IFNγ-secretion by CAR-T cells without target cells; mIgFc, hinge domain of murine immunoglobulin fragment crystallisable; SP, signal peptide; tm, transmembrane region; VH, variable heavy chain; VL, variable light chain.

control mice and mice receiving SP6 CAR T cells displayed continuously increasing B cell numbers in the analysed lymphoid organs spleen, bone marrow and lymph nodes (figure 2A,B, gating in online supplemental figure 2A, online supplemental tables 6 and 7 show mean and p values, respectively). These increasing B cell numbers result presumably from both repopulation after irradiation and bone marrow transplantation, and from B cell stimulation after introduction of the MPO antigen. Peripheral blood B cells displayed a slightly different time-course with a maximal repopulation at 5 weeks but decreasing numbers afterwards (figure 2B). In contrast, mice treated with CD19 CAR T cells showed almost absent B cells in all analysed compartments, which was already evident at 2 weeks and lasted up to 8 weeks (figure 2A,B). Kidney-infiltrating B cells were only assessed at 8 weeks and their number was significantly reduced in CD19 CAR T cell-treated mice compared with mice treated

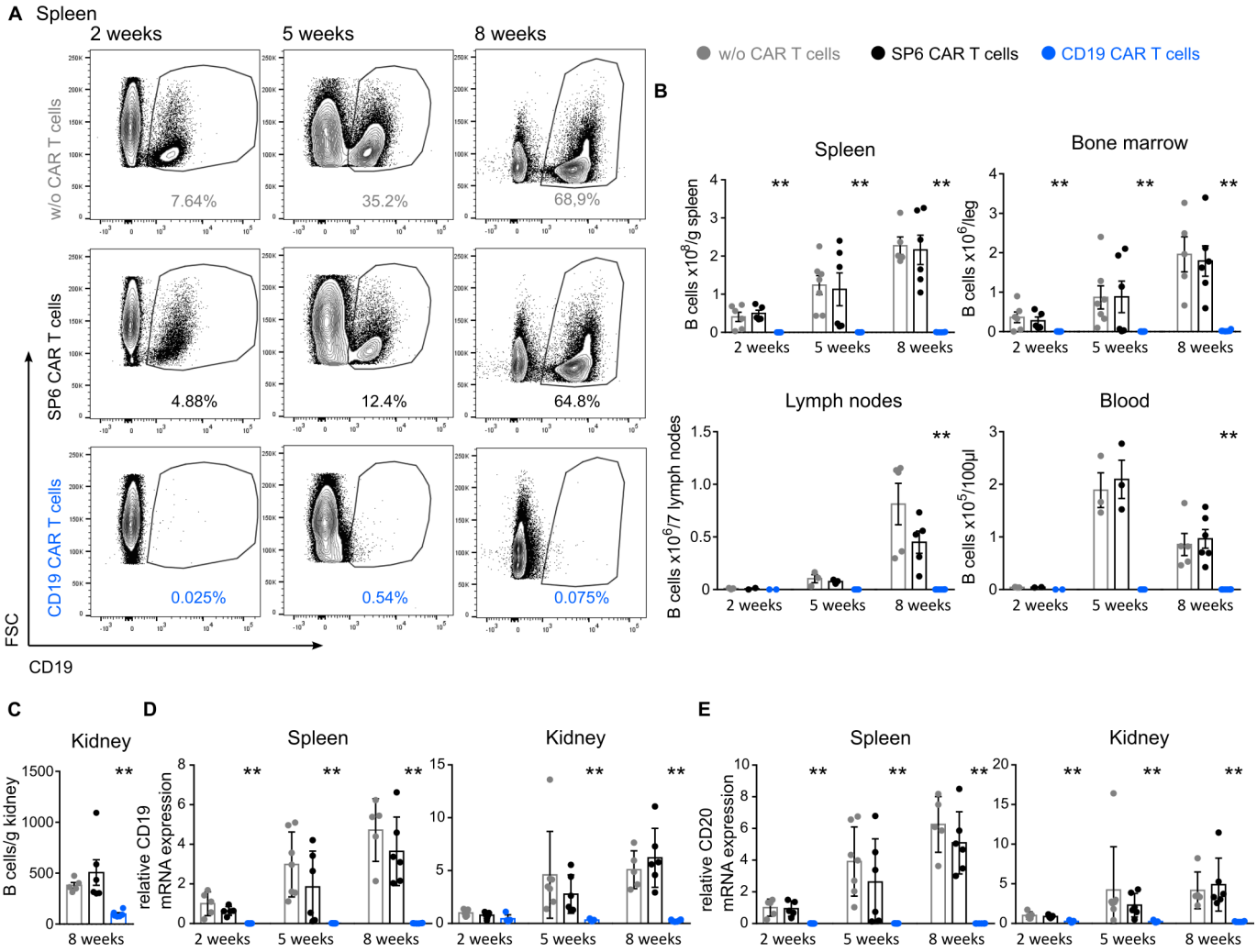

Figure 2 CD19 chimeric antigen receptor (CAR) T cells deplete CD19$^+$ B cells in mice with anti-myeloperoxidase-induced glomerulonephritis. (A) Representative flow-cytometry displaying gated CD19$^+$ B cells in the spleen of controls, SP6 and CD19 CAR-treated mice at 2, 5 and 8 weeks. (B) Numbers of CD19$^+$ B cells in different lymphoid compartments and (C) in the kidneys. (D) Quantification of CD19 and (E) CD20 mRNA by real-time PCR of spleen and kidney samples of control mice, SP6 and CD19 CAR-treated mice at 2, 5 and 8 weeks. Data in (B–E) are represented as individual values and averages with SD. Difference between SP6 and CD19, *p<0.05, **p<0.01. Two independent experiments with a total of 5–7 mice per group were done. Blood and lymph node samples at 2 weeks were only taken from 2 to 3 animals. At 5 weeks only from three animals per group enough cells could be isolated from blood and lymph nodes to analyse B cells.

with SP6 CAR T cells or without CAR T cells (figure 2C). To rule out an unspecific detection issue of CD19 B cells after CD19 CAR T cell treatment as a consequence of antigen-masking or downregulation of CD19 antigen, B cell specific markers were additionally assessed by mRNA quantification. Reduced CD19 (figure 2D) and CD20 (figure 2E) mRNA levels in spleens, which were detected only in mice treated with CD19 CAR T cells, confirmed the flow cytometry data. In the kidneys, both CD19 and CD20 mRNA were reduced from 5 weeks onwards (figure 2D,E). Together, we observed a reduction of CD19 B cells in all analysed compartments lasting up to 8 weeks after treatment with CD19 CAR T cells.

CD19 CAR T cell treatment efficiently decreases plasmablasts

We next investigated whether CD19 CAR T cell treatment reduces plasmablasts and plasma cells as the main sources of MPO-ANCA IgG and crucial drivers of the disease pathogenesis. We assessed B220$^+$ CD138$^-$ plasmablasts, B220$^-$ CD138$^+$ plasma cells, and B220$^+$ CD138$^+$ intermediate plasma cells, respectively (gating depicted in online supplemental figure 2). Mice treated with CD19 CAR T cells showed a rapid, and strong depletion of plasmablasts in spleen, bone marrow and in the kidneys during the 8-week observation period (figure 3A,B, online supplemental tables 8 and 9 show mean and p values, respectively). Intermediate plasma cells were depleted in spleen and bone marrow at all analysed time points, whereas the small number of kidney intermediate plasma cells was not affected (figure 3A,B). Plasma cells were detected in spleen, bone marrow and kidneys. With CD19 CAR T cell treatment, plasma cell numbers were only transiently decreased in the spleen at week 5 but not in bone marrow and kidneys. Lymph nodes and blood displayed decreased numbers of plasmablasts and intermediate plasma cells in mice that received CD19 CAR T cells (online supplemental figure 3). The effective depletion of both plasmablasts and intermediate plasma cells is very likely induced by a direct CD19 CAR T cell-mediated effect as both cell populations displayed strong CD19 antigen expression (96.4%±2.3 of plasmablast display CD19 expression, 82.1%±17.7 of intermediate plasma cells). In contrast, plasma cells did not express CD19 antigen in significant amounts (5.0%±2.3) and were

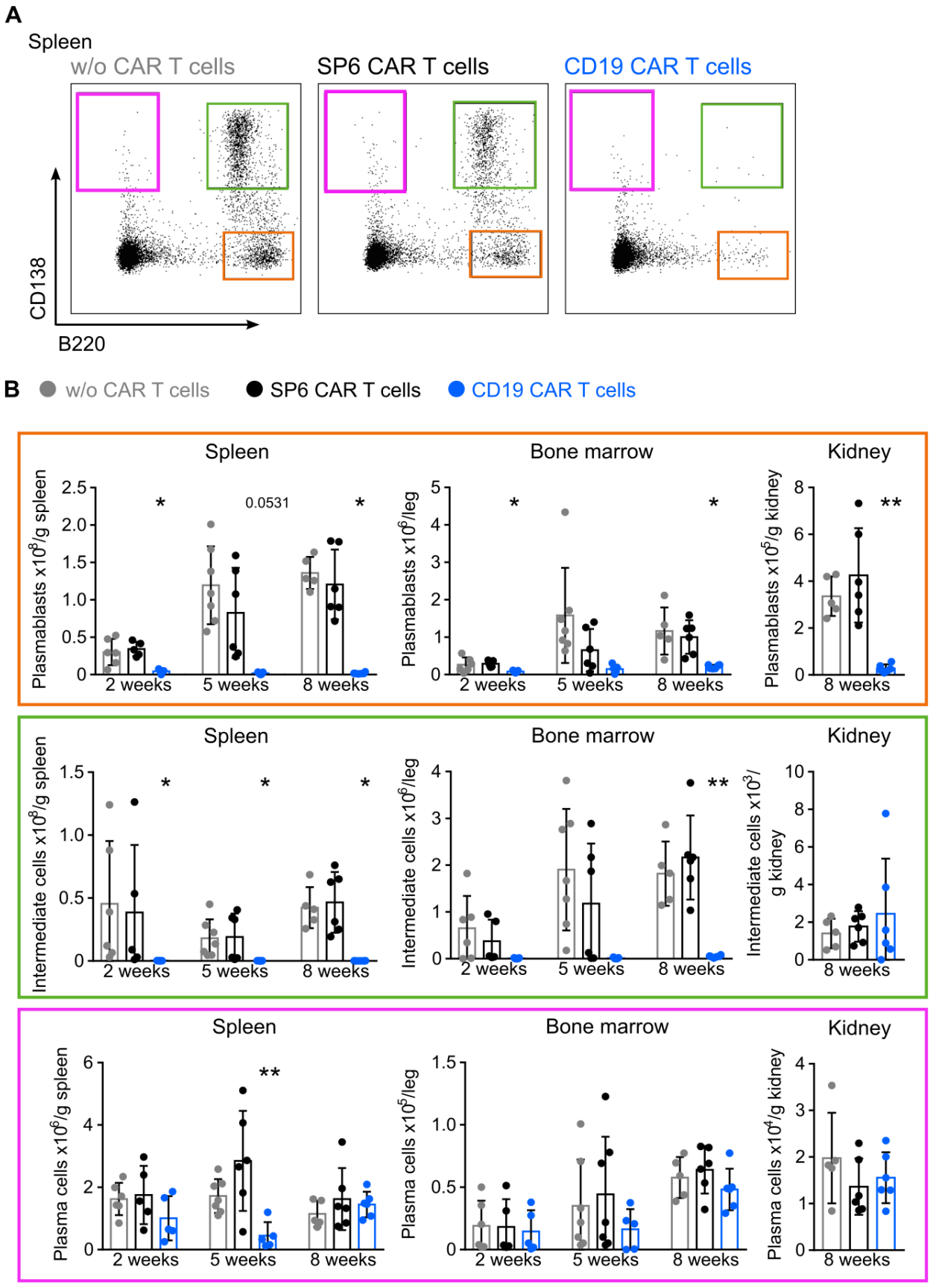

Figure 3 CD19 chimeric antigen receptor (CAR) T cells deplete plasmablasts in mice with anti-myeloperoxidase-induced glomerulonephritis. (A) Representative flow-cytometry displaying detection of plasmablasts (CD138$^-$ B220$^+$, orange), plasma cells (CD138$^+$ B220$^-$, magenta) and intermediate plasma cells (CD138$^+$ B220$^+$, green) in the spleen at 2 weeks. (B) Numbers of plasmablasts, intermediate plasma cells and plasma cells in spleen, bone marrow and kidneys determined by flow cytometry. Data in (B) are represented as individual values and averages with SD. Difference between SP6 and CD19, *p<0.05, **p<0.01. Two independent experiments with a total of 5–7 mice per group were done.

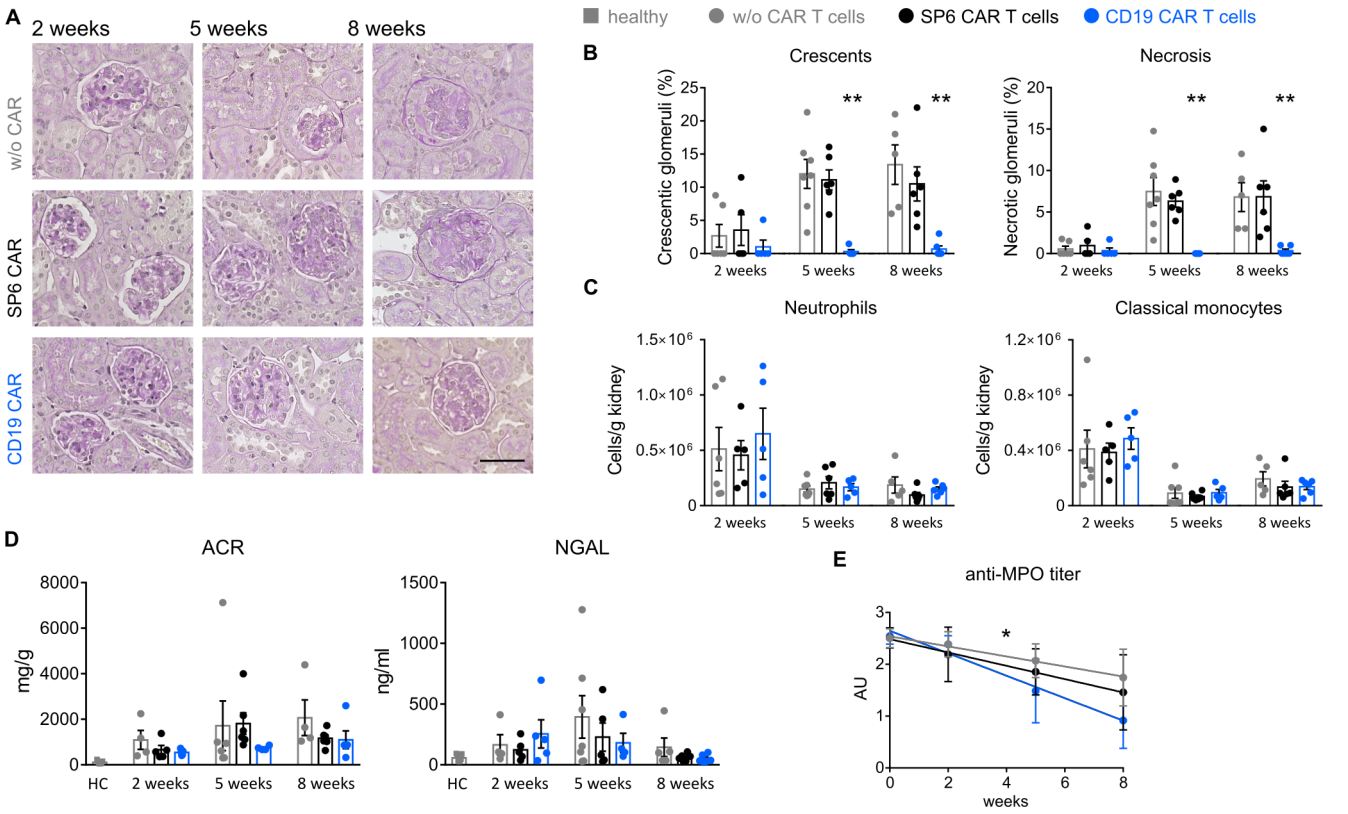

Figure 4 CD19 chimeric antigen receptor (CAR) T cells protect from anti-myeloperoxidase (MPO)-induced glomerulonephritis. (A) Representative kidney histology (PAS reaction) of controls (w/o CAR), SP6 and CD19 CAR-treated mice at 2, 5 and 8 weeks. Glomerular damage with incipient crescent development and hypercellularity at 5 weeks and evident crescents and necrosis at 8 weeks in both control groups is displayed. Scale bar, 50 µm. (B) Quantification of crescent and necrosis formation in the kidneys indicating protection from glomerular damage in CD19 CAR T cell-treated mice. (C) Quantification of kidney-infiltrating neutrophils ($CD45^+$ $CD11b^+$ $Ly6G^+$) and monocytes ($CD45^+$ $CD11b^+$ $Ly6G^-$ $Ly6C^+$) by flow-cytometry. (D) Quantification of albuminuria (albumin to creatinine ratio, ACR) and of urinary neutrophil gelatinase-associated lipocalin as markers of kidney damage, measured by ELISA. Urine samples of n=7 healthy $MPO^{-/-}$ mice (HC, healthy control) are measured for comparison. (E) Determination of anti-MPO titre before irradiation and bone marrow transplantation (week 0) and during disease course (weeks 2, 5, 8) by ELISA. Data in (B–D) are represented as individual values and averages with SD. Data in (E) are represented as averages (circles) with SD. Linear regression analysis (lines) was performed to evaluate differences of slopes. Difference between SP6 and CD19, $^{\#}$difference between control and CD19, $^{*/\#}p<0.05$, $^{**/\#\#}p<0.01$. Two independent experiments with a total of 5–7 mice per group were done.

spared from direct CD19 CAR T cell-mediated depletion (online supplemental figure 4, online supplemental tables 14 and 15 show mean and p values, respectively).

Summarised, CD19 CAR T cells efficiently and persistently depleted B cells, plasmablasts and intermediate plasma cells but not plasma cells in the preclinical model of MPO-ANCA induced crescentic glomerulonephritis.

CD19 CAR T cell treatment protects mice from anti-MPO-induced glomerulonephritis

As B cells and cells of the plasma cell lineage play a central role in ANCA-induced crescentic glomerulonephritis, we next asked whether mice treated with CD19 CAR T cells were protected from renal injury in our preclinical animal model. We observed that both control mice that did not receive CAR T cells and mice treated with SP6 CAR T cells developed kidney injury with similar formation of glomerular crescents and necrosis. In contrast, treatment with CD19 CAR T cells protected mice from NCGN as almost no crescentic or necrotic glomeruli were detected (figure 4A,B, online supplemental tables 10 and 11 show mean and p values, respectively). We did not observe differences in kidney myeloid cell influx with respect to both neutrophils and monocytes (figure 4C). In addition, no difference was found in the influx of macrophages and dendritic cells (online supplemental figure 5, online supplemental tables 16 and 17 show mean and p values, respectively) or T cells (online supplemental figure 6, online supplemental tables 18 and 19 show mean and p values, respectively). Urine damage marker displayed a reduction in albuminuria at 5 weeks and no differences for NGAL in CD19 CAR T cell treated mice (figure 4D). MPO-ANCA titre decrease over the 8-week time period was significantly steeper in CD19 CAR T cell-treated mice compared with both control groups (figure 4E). Peripheral blood cell counts revealed less leucocytes and neutrophils at 5 weeks and diminished lymphocytes at 5 and 8 weeks. No differences were observed for monocytes, eosinophils, erythrocytes, haemoglobin and haematocrit (online supplemental figure 7, online supplemental tables 20 and 21 show mean and p values, respectively).

In conclusion, we established that CD19 CAR T cells protected from acute kidney injury by efficiently depleting B cells, plasmablasts and intermediate plasma cells.

DISCUSSION

We explored the feasibility and protective potential of CD19 CAR T cells in a preclinical model of ANCA-induced autoimmune vasculitis. We observed reliable persistence of CAR T

cells resulting in robust depletion of B cells, plasmablasts and intermediate plasma cells, and progressive MPO-ANCA decline. Importantly, CD19 CAR T cells protected mice from MPO-ANCA induced NCGN. To our knowledge, this is the first report demonstrating high efficacy of CD19 B cell-targeting CAR T cells in an ANCA-induced vasculitis model. Our data may spark future experimental and clinical studies exploring CAR T cell treatments in AAV.

Randomised controlled clinical trials established the B cell-depleting rituximab antibody as an effective treatment in AAV.[9 12] However, up to approximately 25% of AAV patients do not enter complete clinical remission with current standard induction therapies and 30%–50% of those achieving remission develop disease relapses.[11 24 25] Thus, there is an urgent medical need to develop innovative therapeutic approaches for inducing and maintaining disease remission in AAV patients. CD19 CAR T cells may provide such an innovative strategy. In a proof-of-principle study, we tested feasibility and efficacy of CD19 CAR T cells in a preclinical AAV model. We observed strong and persistent depletion of B cells and plasmablasts with CD19 CAR T cell treatment that protected from MPO-ANCA induced glomerulonephritis. The MPO-ANCA levels were significantly, but nevertheless only partly, decreased in mice treated with CD19 CAR T cells. However, treatment resulted in strong protection from disease induction despite incomplete MPO-ANCA depletion, suggesting autoantibody-independent protective effects of CAR T cell-mediated B cell and plasmablast depletion. Indeed, several B cell functions contribute to autoimmune diseases, including autoantibody generation, inflammatory cytokine secretion and autoantigen-presentation to T cells, thereby triggering $CD4^+$ and $CD8^+$ T cell responses. Importantly, and in agreement with our findings, treatment with CD20-depleting antibodies can achieve clinical remission in some autoimmune diseases despite autoantibody persistence underscoring the importance of autoantibody-independent B cell functions.[26] ANCA vasculitis provides an example where ANCA seroconversion is not a *conditio sine qua none* for remission induction by rituximab.[12 27] Additionally, results from animal experiments reinforce the concept that B cells have multiple antibody-independent functions in AAV. Gan *et al* described that anti-CD20 mAb induced B cell apoptosis, increased regulatory T cells, and attenuated T cell-mediated autoimmunity and kidney damage.[28] Moreover, B cells act as antigen-presenting cells thereby promoting T cell responses. Steinmetz *et al* reported B cell infiltrates in kidneys from AAV patients organised as ectopic lymphoid structures.[29] Finally, experimental data show that B cells are important mediators of autoimmunity by modulating myeloid cell functions, for instance via the generation of GM-CSF.[30] Thus, depleting B cells is a promising treatment strategy in AAV with antibody-dependent and antibody-independent protective effects.

Our study has limitations: first, CD19 CAR T cells were transferred at a time-point with already established anti-MPO autoimmunity although but before established disease. A therapeutic approach was beyond the scope of our study. Second, a longer follow-up time is needed to address long-term safety of CAR T cells. We believe that our data provide a proof-of-concept and a starting point to explore these and additional questions in future studies.

Although B cell depletion by rituximab has improved clinical outcomes in AAV patients, we envision several advantages of CD19-targeting CAR T cells over B cell-depleting antibodies. First, CD19 CAR T cells were highly efficient and depleted B cells (nearly) completely. In contrast, high-sensitive flow cytometry shows residual B cells, including ANCA-specific memory B cells at all time-points after rituximab administration in AAV patients.[31] Second, we found that CD19 CAR T cells engrafted in lymphoid organs and inflamed target organs, such as kidneys. This finding provides an advantage over B cell-targeting antibodies that result in incomplete tissue B cell depletion.[32] Both effects have the potential to improve outcomes in AAV patients refractory to conventional therapies, similarly to what was recently demonstrated in difficult-to-treat and therapy-refractory lupus patients.[21] Moreover, it was shown that B cells from lymphoma patients treated with rituximab lost surface and cytoplasmic CD20 expression at relapse. Because the CD19 CAR T cells recognise an antigen different than CD20 on the B cell-surface, CD19 CAR T cells have the potential to deplete B cells even after they lost the CD20 antigen during rituximab treatment.

In addition, CD19 CAR T cells could be of value in patients with repeated clinical relapses requiring repetitive treatment cycles. Third, CD19 CAR T cells may provide a strategy to achieve drug-free long-term disease remission. It was recently demonstrated in one CD19 CAR T cell-treated lupus patient that B cells reappeared but displayed a naïve phenotype. This observation supports the notion that these reprogrammed B cells lost their autoimmune potential making remission maintenance treatment unnecessary.[21] AAV could provide another example of an autoimmune disease suitable for CD19 CAR T cell treatment. However, it is important to first test such an approach in a preclinical disease model. We believe that our proof-of-principle data from a murine MPO-AAV disease model encourages future CAR T cell studies in AAV, including testing CAR T cells after disease onset, and developing antigen-specific CAR T cell approaches. AAV with uniquely characterised autoantigens provides an opportunity for MPO-specific or PR3-specific B cell depletion. The development of chimeric autoantibody receptor T cells would then enable long-lasting and specific depletion of ANCA-generating B cells. However, a CD19 CAR T cell therapy is potentially associated with some disadvantages. First, no long-term safety data regarding CAR T therapy in autoimmune disease exists. Second, adverse reactions such as cytokine release syndrome can appear. Third, the still not antigen-specific, long-lasting and deeper immunosuppression provides a potential risk for infectious complications. Finally, recent reports of the development of T cell lymphomas in patients treated with BCMA-directed or CD19-directed genetically modified autologous CAR T cells lead to an FDA safety alert.[33] This alert illustrates the importance of careful preclinical testing of such innovative novel therapies especially in patients with autoimmune disease as AAV.

Altogether, our data support a direct pathogenic role of B cells in the pathogenesis of AAV and implicate CD19-targeting CAR T cells as a highly efficient strategy to protect from ANCA-induced vasculitis and NCGN. Future improvements of this therapeutic principle may lead to an induction and maintenance of drug-free disease remission in AAV patients.

Acknowledgements We thank Susanne Rolle and Sylvia Lucke for excellent technical assistance.

Contributors UEH and AS conceived and designed the study. UEH, AS, MZ and DL planned and guided experiments. DL, MZ, MB, AR and JS performed experiments. UEH, AS, RK and DL wrote the manuscript, and all authors revised the manuscript and approved the final version. AS acts as guarantor.

Funding This work was supported by grant SCHR 771/8-1 and SCHR 771/10-1 from the Deutsche Forschungsgemeinschaft to AS, grant 394046635—SFB 1365 from the Deutsche Forschungsgemeinschaft to RK and AS, and ECRC grants to AS and RK. UEH was funded by grants from the HGF 'Zukunftsthema Inflammation & Immunology' (2410085).

Competing interests None declared.

Patient and public involvement Patients and/or the public were not involved in the design, or conduct, or reporting, or dissemination plans of this research.

Patient consent for publication Not applicable.

Ethics approval All animal experiments were approved by the local authorities (Landesamt für Gesundheit und Soziales, Berlin, Germany, G0040/20) and followed the ARRIVE (Animal Research: Reporting of In Vivo Experiments) guidelines.

Provenance and peer review Not commissioned; externally peer reviewed.

Data availability statement Data are available upon reasonable request.

ORCID iD

Adrian Schreiber http://orcid.org/0000-0003-1244-6379

REFERENCES

1 Kitching AR, Anders H-J, Basu N, *et al*. ANCA-associated vasculitis. *Nat Rev Dis Primers* 2020;6:71.
2 Schreiber A, Choi M. The role of neutrophils in causing antineutrophil cytoplasmic autoantibody-associated vasculitis. *Curr Opin Hematol* 2015;22:60–6.
3 Rousselle A, Sonnemann J, Amann K, *et al*. CSF2-dependent monocyte education in the pathogenesis of ANCA-induced glomerulonephritis. *Ann Rheum Dis* 2022;81:1162–72.
4 Rousselle A, Kettritz R, Schreiber A. Monocytes promote crescent formation in anti-myeloperoxidase antibody-induced glomerulonephritis. *Am J Pathol* 2017;187:1908–15.
5 Krebs CF, Reimers D, Zhao Y, *et al*. Pathogen-induced tissue-resident memory Th17 (Trm17) cells amplify autoimmune kidney disease. *Sci Immunol* 2020;5:eaba4163.
6 Xiao H, Heeringa P, Hu P, *et al*. Antineutrophil cytoplasmic autoantibodies specific for myeloperoxidase cause glomerulonephritis and vasculitis in mice. *J Clin Invest* 2002;110:955–63.
7 Schreiber A, Xiao H, Falk RJ, *et al*. Bone marrow-derived cells are sufficient and necessary targets to mediate glomerulonephritis and vasculitis induced by anti-myeloperoxidase antibodies. *J Am Soc Nephrol* 2006;17:3355–64.
8 Ooi JD, Chang J, Hickey MJ, *et al*. The immunodominant myeloperoxidase T-cell EPITOPE induces local cell-mediated injury in antimyeloperoxidase glomerulonephritis. *Proc Natl Acad Sci U S A* 2012;109:E2615–24.
9 Jones RB, Tervaert JWC, Hauser T, *et al*. Rituximab versus cyclophosphamide in ANCA-associated renal vasculitis. *N Engl J Med* 2010;363:211–20.
10 Jayne DRW, Merkel PA, Bekker P. Avacopan for the treatment of ANCA-associated vasculitis. *N Engl J Med* 2021;384:599–609.
11 Specks U, Ikle D, Stone JH. Efficacy of remission-induction regimens for ANCA-associated vasculitis. *N Engl J Med* 2013;369:1865–6.
12 Stone JH, Merkel PA, Spiera R, *et al*. Rituximab versus cyclophosphamide for ANCA-associated vasculitis. *N Engl J Med* 2010;363:221–32.
13 de Groot K, Harper L, Jayne DRW, *et al*. Pulse versus daily oral cyclophosphamide for induction of remission in antineutrophil cytoplasmic antibody-associated vasculitis: a randomized trial. *Ann Intern Med* 2009;150:670–80.
14 Pagnoux C, Hogan SL, Chin H, *et al*. Predictors of treatment resistance and relapse in antineutrophil cytoplasmic antibody-associated small-vessel vasculitis: comparison of two independent cohorts. *Arthritis Rheum* 2008;58:2908–18.
15 Smith RM, Jones RB, Guerry M-J, *et al*. Rituximab for remission maintenance in relapsing antineutrophil cytoplasmic antibody-associated vasculitis. *Arthritis Rheum* 2012;64:3760–9.
16 Rhodes JM, Schuster SJ. Chimeric antigen receptor T cells in chronic lymphocytic leukemia: are we any closer to a cure. *Cancer J* 2019;25:436–41.
17 Kochenderfer JN, Wilson WH, Janik JE, *et al*. Eradication of B-lineage cells and regression of lymphoma in a patient treated with autologous T cells genetically engineered to recognize CD19. *Blood* 2010;116:4099–102.
18 Brentjens RJ, Davila ML, Riviere I, *et al*. CD19-targeted T cells rapidly induce molecular remissions in adults with chemotherapy-refractory acute lymphoblastic leukemia. *Sci Transl Med* 2013;5:177ra38.
19 Kansal R, Richardson N, Neeli I, *et al*. Sustained B cell depletion by CD19-targeted CAR T cells is a highly effective treatment for murine lupus. *Sci Transl Med* 2019;11:eaav1648.
20 Mougiakakos D, Krönke G, Völkl S, *et al*. CD19-targeted CAR T cells in refractory systemic lupus erythematosus. *N Engl J Med* 2021;385:567–9.
21 Mackensen A, Müller F, Mougiakakos D, *et al*. Anti-CD19 CAR T cell therapy for refractory systemic lupus erythematosus. *Nat Med* 2022;28:2124–32.
22 Chmielewski M, Abken H. CAR T cells releasing IL-18 convert to T-Bethigh FoxO1Low effectors that exhibit augmented activity against advanced solid tumors. *Cell Reports* 2017;21:3205–19.
23 Kochenderfer JN, Feldman SA, Zhao Y, *et al*. Construction and preclinical evaluation of an anti-CD19 Chimeric antigen receptor. *J Immunother* 2009;32:689–702.
24 Charles P, Terrier B, Perrodeau É, *et al*. Comparison of individually tailored versus fixed-schedule rituximab regimen to maintain ANCA-associated vasculitis remission: results of a multicentre. *Ann Rheum Dis* 2018;77:1143–9.
25 Guillevin L, Pagnoux C, Karras A, *et al*. Rituximab versus azathioprine for maintenance in ANCA-associated vasculitis. *N Engl J Med* 2014;371:1771–80.
26 Cornec D, Avouac J, Youinou P, *et al*. Critical analysis of rituximab-induced serological changes in connective tissue diseases. *Autoimmun Rev* 2009;8:515–9.
27 Smith RM, Jones RB, Specks U, *et al*. Rituximab as therapy to induce remission after relapse in ANCA-associated vasculitis. *Ann Rheum Dis* 2020;79:1243–9.
28 Gan P-Y, Dick J, O'Sullivan KM, *et al*. Anti-CD20 mAb-induced B cell apoptosis generates T cell regulation of experimental myeloperoxidase ANCA-associated vasculitis. *J Am Soc Nephrol* 2021;32:1071–83.
29 Steinmetz OM, Velden J, Kneissler U, *et al*. Analysis and classification of B-cell infiltrates in lupus and ANCA-associated nephritis. *Kidney Int* 2008;74:448–57.
30 Li R, Rezk A, Miyazaki Y, *et al*. Proinflammatory GM-CSF-producing B cells in multiple sclerosis and B cell depletion therapy. *Sci Transl Med* 2015;7:310ra166.
31 van Dam LS, Oskam JM, Kamerling SWA, *et al*. Highly sensitive flow cytometric detection of residual B-cells after rituximab in anti-neutrophil cytoplasmic antibodies-associated vasculitis patients. *Front Immunol* 2020;11:566732.
32 Zhang Z, Xu Q, Huang L. B cell depletion therapies in autoimmune diseases: monoclonal antibodies or chimeric antigen receptor-based therapy. *Front Immunol* 2023;14:1126421.
33 FDA investigating serious risk of T-cell malignancy following BCMA-directed or CD19-directed autologous chimeric antigen receptor (CAR) T cell Immunotherapies. n.d. Available: https://www.fda.gov/vaccines-blood-biologics/safety-availability-biologics/fda-investigating-serious-risk-t-cell-malignancy-following-bcma-directed-or-cd19-directed-autologous